JOURNAL OF VIROLOGY, Oct. 1993, p. 6110–6118
0022-538X/93/106110-09$02.00/0

Vol. 67, No. 10

Deletion Mapping of a Mouse Hepatitis Virus Defective Interfering RNA Reveals the Requirement of an Internal and Discontiguous Sequence for Replication

YI-JYUN LIN[1] AND MICHAEL M. C. LAI[1,2]*

Howard Hughes Medical Institute[2] and Department of Microbiology,[1] University of Southern California School of Medicine, Los Angeles, California 90033-1054

Received 21 April 1993/Accepted 26 June 1993

All of the defective interfering (DI) RNAs of mouse hepatitis virus (MHV) contain both the 5′ and 3′ ends of the viral genomic RNA, which presumably include the *cis* sequences required for RNA replication. To define the replication signal of MHV RNA, we have used a vaccinia virus-T7 polymerase-transcribed MHV DI RNA to study the effects of sequence deletion on DI RNA replication. Following infection of susceptible cells with a recombinant vaccinia virus expressing T7 RNA polymerase, various cDNA clones derived from a DI RNA (DIssF) of the JHM strain of MHV, which is a 3.5-kb naturally occurring DI RNA, behind a T7 promoter were transfected. On superinfection with a helper MHV, the ability of various DI RNAs to replicate was determined. Serial deletions from the middle of the RNA toward both the 5′ and 3′ ends demonstrated that 859 nucleotides from the 5′ end and 436 nucleotides from the 3′ end of the MHV RNA genome were necessary for RNA replication. Surprisingly, an additional stretch of 135 nucleotides located at 3.1 to 3.3 kb from the 5′ end of the genome was also required. This stretch is discontiguous from the 5′-end *cis* replication signal and is present in all of the naturally occurring DI RNAs studied so far. The requirement for a long stretch of 5′- and 3′-end sequences predicts that the subgenomic MHV mRNAs cannot replicate. The efficiency of RNA replication varied with different cDNA constructs, suggesting possible interaction between different regions of DI RNA. The identification of MHV RNA replication signals allowed the construction of an MHV DI-based expression vector, which can express foreign genes, such as the chloramphenicol acetyltransferase gene.

A viral genome contains, in addition to various open reading frames (ORFs) encoding viral proteins, sequences for gene regulation, genome packaging, and genome replication. These *cis*-acting elements usually have specific sequences and/or structures which are recognized by host factors or viral gene products. The sequences which are recognized by polymerase and are required to support genome replication can be viewed as the replication signal. The replication of a viral genomic RNA is accomplished through cycling at least two phases: from genomic sense to antigenomic sense (template-preparing phase) and from antigenomic sense back to genomic sense (genome-amplifying phase). Therefore, the replication signals of the genomes of linear RNA viruses probably include both 5′ and 3′ ends of the genome, since the replication of either strand of RNA must initiate at one end, proceed to the other end, and reinitiate there.

Mouse hepatitis virus (MHV) is a prototype coronavirus, containing a linear, single-stranded, nonsegmented, positive-sense RNA of approximately 31 kb (12, 13, 28). The virion is composed of three or four structural proteins. The viral envelope contains the spike (S) protein and membrane (M) protein. In some strains, there is an additional protein, the hemagglutinin-esterase (HE), in the envelope (36). The nucleocapsid (N) protein interacts with the viral genomic RNA (33) and forms a helical nucleocapsid inside the virion. During MHV infection of susceptible cells, seven or eight mRNAs ranging in size from 31 to 1.8 kb are transcribed. These mRNAs are 3′-coterminal with the genomic RNA and have a nested-set structure (11), and all of them contain a leader sequence of approximately 70 nucleotides at the 5′ end (11). All of the mRNAs, except mRNA 7, have more than one ORF, but only the 5′-most ORF of each mRNA is translated into proteins (14, 32). For instance, S protein is translated only from mRNA 3, and N and M proteins are translated from mRNAs 6 and 7, respectively. Viral RNA polymerase is presumably translated from mRNA 1 (11).

RNA replication represents an important process in the replication cycle of MHV, and the replication signal is a key to the investigation of RNA replication. However, this issue remained largely unaddressed in the past. One main obstacle is that the large size of the MHV genome makes it difficult to specifically alter the sequence of the genomic RNA. The recent success in the synthesis of replicating defective interfering (DI) RNAs of MHV (19, 23) has made this question more amenable to experimental analysis. DI RNAs are deletion mutant RNAs that interfere with the replication of viral genomic RNA in the cell. When MHV was serially passaged at a high multiplicity of infection in cell culture, a variety of DI RNAs of different sizes were detected (18, 22). All of the DI RNAs can replicate in the presence of proper helper viruses, indicating that the replication signal is included in the DI RNAs. These DI RNAs generally have multiple deletions but always retain both the 5′ and 3′ ends of viral genomic sequences (20, 21, 23, 34). For instance, the two smallest naturally occurring DI RNAs of the JHM strain of MHV, DIssE and DIssF, with sizes of 2.2 and 3.5 kb, respectively, contain approximately 0.9 kb from the 5′ end of the viral genome and 0.6 and 0.45 kb, respectively, from the 3′ end (21, 23). In addition, the middle of DIssF contains three discontiguous regions (domains II, III, and IV) derived from internal gene 1 sequences, whereas DIssE has only one middle domain, which overlaps with domain II of DIssF (23).

* Corresponding author.

Most of the sequences shared between DIssE and DIssF are also retained in a DI RNA of the A59 strain of MHV (34). It stands to reason that the replication signal of DI RNA is included in the sequences shared by DIssE and DIssF and that the sequences unique to either one, such as domains III and IV of DIssF, are not essential for RNA replication. To define the minimum sequence required for RNA replication, ideally one should use the smallest DI RNA (e.g., DIssE) and progressively delete nonessential sequences. However, preliminary attempts at deleting any region of DIssE RNA sequence always destroyed the replicating ability of RNA. Therefore, we used a larger DI RNA, DIssF, and performed nested-set deletions from the middle, which is not present in DIssE RNA, toward both the 5′ and 3′ ends of the RNA. We used vaccinia virus-T7 polymerase-transcribed MHV DI RNAs and studied the effects of deletion of DI sequence on RNA replication. By this approach, we defined the essential replication signal for this DI RNA. Our results showed that MHV DI RNA requires surprisingly long stretches of sequence at both the 5′ and 3′ ends and also a discontiguous region located at more than 3 kb from the 5′ end. The efficiency of RNA replication varied with different RNA constructs, suggesting that the interaction between sequences within the DI RNA may modulate RNA replication. The potential for developing an MHV DI RNA-based expression vector is also demonstrated.

MATERIALS AND METHODS

Viruses and cells. The A59 strain (24) of MHV and T7 RNA polymerase-recombinant vaccinia virus, vTF7-3 (3) (kindly provided by B. Moss, National Institutes of Health, Bethesda, Md.), were used throughout this study. All of the experiments were performed with DBT cells, a murine astrocytoma cell line (5), which is susceptible to both MHV and vaccinia virus infection. The vTF7-3 virus stock was prepared as previously described (17).

Construction of serial deletion clones. To obtain 5′-end deletion clones, 7.5 μg of plasmid DF1-1 (23), which is the cDNA clone of DIssF, was first digested with *Bss*HII and *Nsi*I (see Fig. 2A) and then progressively deleted into the 5′ end by using the Erase-a-Base system (Promega) as specified by the manufacturer. Briefly, the restriction enzyme-digested plasmid DNA was treated with exonuclease III for 1 to 12 min at room temperature, an aliquot of the reaction mixture was removed at 1-min intervals, and the reaction was stopped immediately after removal. The digested DNA was made blunt ended by treatment with S1 nuclease and Klenow enzyme as suggested by the manufacturer (Promega). The resulting DNA was self-ligated with T4 DNA ligase and transformed into *Escherichia coli* DH5α. To obtain 3′-end deletion clones, 7.5 μg of DF1-1 DNA was digested with *Nsi*I and *Acc*I (see Fig. 3A) and progressively deleted into the 3′ end by the same procedures as described above, except that the exonuclease III reactions were carried out for 1 to 8 min. All of the clones obtained were sequenced across the junction points with an upstream and a downstream primer by using the Sequenase system (U.S. Biochemical).

Construction of plasmids. (i) **ADI-2.** DF1-1 DNA was digested with *Pvu*I, treated with T4 DNA polymerase, and then digested with *Eco*RI. The 0.45-kb *Pvu*I-*Eco*RI fragment representing the 3′ end of DIssF RNA was inserted into *Sma*I-*Eco*RI sites of pGem-3Zf(−) (Promega) to generate pGem-DF3′. The 1.1-kb *Hin*dIII-*Sph*I fragment containing T7 promoter and the 5′ end of DIssF was inserted into the *Hin*dIII and *Sph*I sites of pGem-DF3′, yielding plasmid ADI-2. For the structure of the ADI-2 cDNA, see Fig. 5A.

(ii) **DF-IRES-CAT and DF-SERI-CAT.** A DNA fragment containing the ORF of the chloramphenicol acetyltransferase (CAT) gene was made by polymerase chain reaction, in which pCAT-Basic (Promega) plasmid DNA was mixed with oligonucleotide primers LA578 (5′-ATGGAGAAAA AAATCACTGG-3′) and LA579 (5′-TTACGCCCCGCCCTG CCACT-3′) and *Taq* DNA polymerase (Boehringer Mannheim Biochemicals). Polymerase chain reaction was carried out for 30 cycles of 1 min at 94°C, 1 min at 58°C, and 3 min at 72°C. The amplified CAT DNA was made blunt ended and inserted into *Sal*I-linearized ADI-2 which had been made blunt ended with Klenow enzyme, yielding AF3-CAT. The internal ribosomal entry site (IRES) sequence of encephalomyocarditis virus (EMCV) (6) was obtained from the pTM1 vector (27) by digestion with *Apa*I and *Nco*I and blunt ending with T4 DNA polymerase. The DNA fragment containing the IRES sequence was inserted into *Pst*I-linearized AF3-CAT, which had been made blunt ended with T4 DNA polymerase, in both sense and antisense orientations to generate AF3-IRES-CAT and AF3-SERI-CAT, respectively. These two plasmids were then used as templates for PCR amplification, in which oligonucleotide primers LA52 (5′-AAGCTTAATACGACTCACTATAGTATAAGAGTGA TTGGCGTCCGTAC-3′) and LA579 were used to amplify IRES-CAT and SERI-CAT sequences. The amplified DNAs were made blunt ended, digested with *Sph*I, and then inserted into *Sph*I-*Acc*I-digested DF1-1, resulting in DF-IRES-CAT and DF-SERI-CAT.

Virus infection, DNA transfection, and RNA labeling in vivo. The experimental protocol was modified from the published procedures (30). Approximately 5×10^5 DBT cells in 60-mm plates were infected with vTF7-3 at a multiplicity of infection of 5. Two hours later, the infected cells were washed with serum-free Eagle's minimum essential medium (MEM; GIBCO-BRL), and 5 μg of *Xba*I-linearized plasmid DNA was transfected into the infected cells by using *N*-[1-(2,3-dioleoxyloxy)propyl]-*N*,*N*,*N*,-trimethylammonium methyl sulfate (DOTAP) reagent by the procedure recommended by the manufacturer (Boehringer Mannheim Biochemicals). Cells were incubated for 10 h at 37°C and then superinfected with A59 virus at a multiplicity of infection of 10. After 1 h of virus adsorption, the cells were washed with MEM, and 1 ml of labeling medium (MEM containing 10 μg of actinomycin D [Sigma] per ml, 100 μCi of [^{3}H]uridine [Dupont NEN] per ml, 2% fetal bovine serum [Irvine Scientific]) was added. The infected cells were incubated for an additional 11 h at 37°C, and the intracellular RNA was extracted by a previously published method (20, 23). To harvest virus for subsequent passages, MEM containing 3% newborn bovine serum (Irvine Scientific) and 10 μg of actinomycin D per ml without [^{3}H]uridine was used after A59 superinfection. The supernatant was collected 14 h after A59 infection. Half of the supernatant was used directly to infect approximately 5×10^5 DBT cells. The infected cells were washed with MEM at 1 h postinfection (p.i.), and 1 ml of the labeling medium was added to the cells. The intracellular RNA was extracted at 8 h p.i.

RNA electrophoresis. [^{3}H]uridine-labeled RNA was denatured with 1 M glyoxal and separated by electrophoresis on a 1% agarose gel (25). After electrophoresis, gels were treated with En^{3}Hance (Dupont) by following the protocol provided by the manufacturer, dried, and exposed to X-ray films.

CAT assay. Approximately 5×10^5 cells were washed five

times with cold phosphate-buffered saline, and then 0.25 ml of cold NTE (100 mM NaCl, 10 mM Tris-HCl [pH 8.0], 1 mM EDTA) buffer was added. The cells were scraped off with a rubber policeman, pelleted, resuspended in 150 μl of 0.25 M Tris-HCl (pH 8.0) buffer, and subjected to three freeze-thaw cycles. The cell extract was centrifuged, and the supernatant was recovered and heated at 60°C for 10 min. Cell extract (50 μl) was mixed with 65 μl of 0.25 M Tris-HCl (pH 8.0), 4 μl of [^{14}C]chloramphenicol (0.025 mCi/ml [Dupont NEN]), and 5 μl of *n*-butyryl coenzyme A (5 mg/ml; Sigma) and incubated at 37°C for 15 h. The reaction mixture was extracted with 300 μl of xylenes. The upper layer (xylenes) was recovered and back-extracted twice with water. Then 200 μl of the upper layer was mixed with 4 ml of ScintiVerse BD (Fisher Scientific) and the ^{14}C count was measured.

RESULTS

Establishment of a sensitive assay system to detect DI RNA replication. Previous studies of MHV DI RNA replication or transcription usually employed in vitro-transcribed DI RNA to transfect virus-infected cells (termed passage 0 [P0] cells); the released virus was then used to infect another set of cells (passage 1 [P1] cells) (7, 19, 23, 34). By using this approach, DI RNA could be detected generally in P1 cells but only occasionally in P0 cells. Because of the potential occurrence of recombination between DI RNA and helper virus RNA (4, 9, 10, 35), the RNA detected in P1 cells may not represent the original DI RNA. To develop a more sensitive assay method to overcome this potential problem, we chose to use a recombinant vaccinia virus encoding T7 RNA polymerase (3). In this system, DBT cells were infected with T7 RNA polymerase-recombinant vaccinia virus, vTF7-3 (3). At 2 h after vTF7-3 infection, *Xba*I-linearized DF1-1 plasmid DNA, which contains DIssF cDNA behind a T7 promoter, was transfected. The in vitro-transcribed DIssF RNA contained only one extra nucleotide (G) at its 5′ end but 11 extra nucleotides at its 3′ end, which are derived from the cloning vector. Following incubation at 37°C for 10 h, cells were superinfected with MHV-A59 to provide viral gene products necessary for DI RNA replication. Actinomycin D and [^{3}H]uridine were added to the medium to label newly synthesized MHV RNAs but not vaccinia virus RNA. Under these conditions, radiolabeled MHV DI RNA (3.6 kb) and seven MHV A59-specific mRNAs were readily detected in P0 cells (Fig. 1, lane 4). The authenticity of this DI RNA replication system was supported by the finding that DIssF RNA was not detected when either A59 or vTF7-3 was omitted (Fig. 1, lanes 2 and 3). In addition, RNA synthesis by vTF7-3 was completely abrogated after the addition of actinomycin D (Fig. 1, compare lanes 1 and 2), indicating that RNA synthesis detected in the presence of actinomycin D in A59-superinfected cells represented MHV-specific RNA synthesis. These results, taken together, indicated that [^{3}H]uridine-labeled RNA represented DI RNA replication mediated by helper MHV but not the primary transcription products synthesized by vTF7-3-induced T7 RNA polymerase. Thus, the extra sequences at the 5′ and 3′ ends of DF1-1 RNA did not interfere with RNA replication. This system was used to determine the replicating ability of various DI constructs described below.

Replication signal at the 5′-end of DI RNA. Because the sequences required for RNA replication are expected to include both 5′ and 3′ ends of DI RNA, we constructed nested-set deletion mutants with deletions starting from the middle of DI RNA and extending toward both ends. These

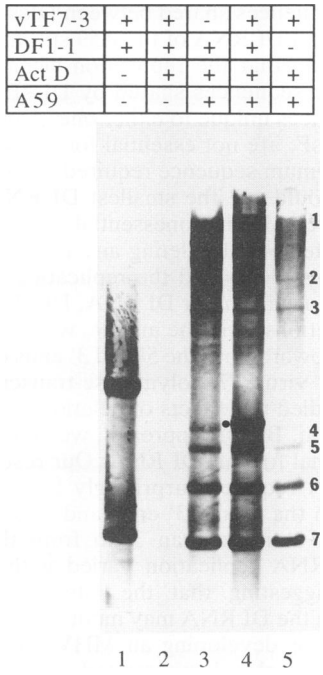

FIG. 1. Electrophoresis of [^{3}H]uridine-labeled viral RNAs. Intracellular RNAs were analyzed by electrophoresis on a 1% agarose gel, incubated with En^{3}Hance, dried, and exposed to X-ray films for 12 to 24 h. vTF7-3 and A59 virus infection and DNA transfection to DBT cells were performed as indicated above each lane. The seven A59-specific mRNAs are indicated by numbers. The dot indicates DIssF RNA. Lane 1 contained one-fifth the amount of RNA found in other lanes. Radiolabeled bands in lane 1 represent cellular RNA, vTF7-3-specific RNA, and T7-transcribed DF1-1 RNA. DF1-1 RNA could not be seen in lane 1 because of high background.

mutants were tested for their ability to replicate in the recombinant vaccinia virus-T7 polymerase system. Since domains III and IV of DIssF are not present in DIssE (23), we reasoned that these two domains were not part of the replication signal of DI RNA and could be deleted without affecting replication. Therefore, the fragment (0.7 kb) spanning from the *Bss*HII site in domain II to the *Nsi*I site in domain III of DIssF cDNA was deleted first. The remaining DNA was treated with exonuclease III for various lengths of time to delete unidirectionally from the *Bss*HII site toward the 5′ terminus. The resulting clones containing different degrees of deletion were studied for their abilities to replicate by metabolic labeling with [^{3}H]uridine and separation by agarose gel electrophoresis. Since some of the DI RNAs are very close in size to viral mRNAs, their identification under standard electrophoresis conditions was sometimes difficult. In these cases, electrophoresis was also performed for a longer period to achieve a clear separation of DI RNAs from viral mRNAs (Fig. 2B). The genetic structures of the deletion clones are shown in Fig. 2A. Among these constructs, DF5′Δ0-4, DF5′Δ6-2, and DF5′Δ6-9 yielded [^{3}H]uridine-labeled RNAs of the respective expected sizes in P0 cells, although their efficiencies of replication differed (Fig. 2B). DF5′Δ7-4 RNA was barely detectable in P0 cells but could be detected occasionally in some experiments (data not shown). In contrast, clones DF5′Δ7-5, DF5′Δ7-7, DF5′Δ7-11, DF5′Δ7-12, DF5′Δ9-6, and DF5′Δ10-1 did not yield any DI RNA (Fig. 2B; data not shown). To determine whether any of the apparently nonreplicating RNAs de-

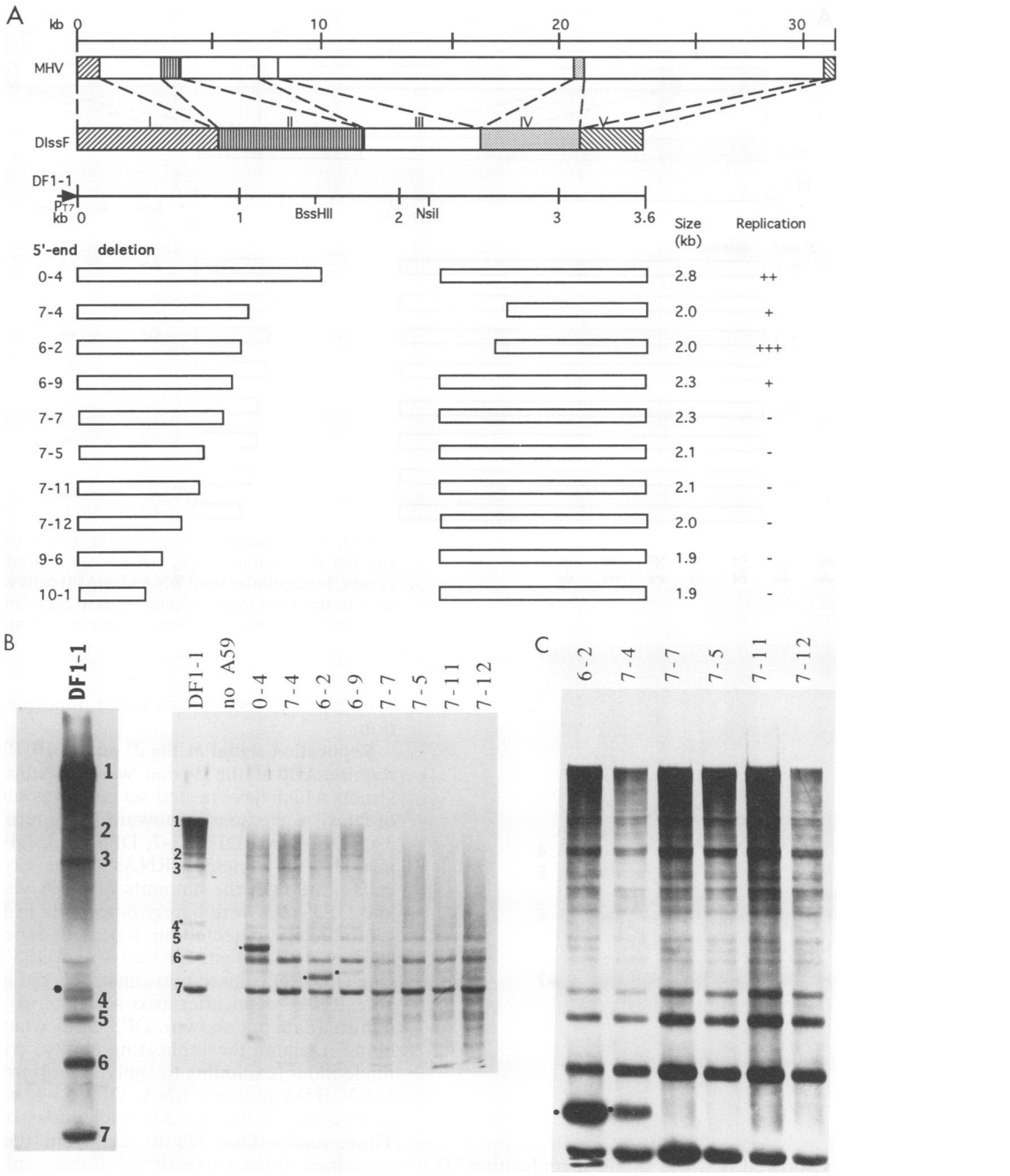

FIG. 2. Replication of 5′-deletion clones. (A) Structure of DIssF and the 5′-deletion clones. The RNA size and relative replication efficiency of each clone are summarized on the right. (B) Electrophoresis of intracellular viral RNAs derived from P0 cells transfected with the 5′-deletion clones. Viruses and DNAs were added as indicated. Actinomycin D was added in all lanes. Two different runs of intracellular viral RNAs from DF1-1-transfected P0 cells are shown. A59-specific mRNAs are indicated by numbers. (C) Electrophoresis of intracellular viral RNAs from P1 cells. Viruses released from P0 cells were used to infect a new set of cells. Intracellular viral RNAs from P1 cells were analyzed. Dots indicate DI RNAs.

scribed above might replicate to a small extent and thus could be detected after one round of virus passage, which has been shown to amplify DI RNA (19, 20), viruses released from P0 cells were used to infect a new set of DBT cells, and intracellular viral RNA (P1 cells) was analyzed (Fig. 2C; data not shown). Both DF5′Δ6-2 and DF5′Δ7-4 could be detected in large quantities, even though the replication efficiency of DF5′Δ7-4 was low in P0 cells (Fig. 2B), suggesting that virus passages amplified DI RNA replication. None of the other nonreplicating clones, however, synthesized any detectable DI RNA in P1 cells, indicating that they are completely devoid of any replicating ability. Some mutant DI RNAs, e.g., DF5′Δ6-2, replicated more efficiently than did other clones of comparable size (Fig. 2B). Sequence analysis of

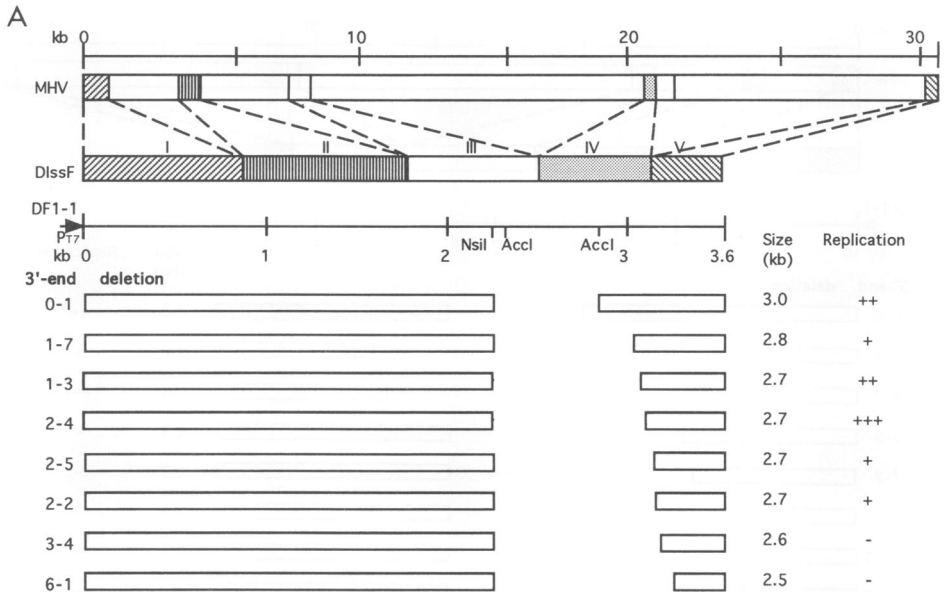

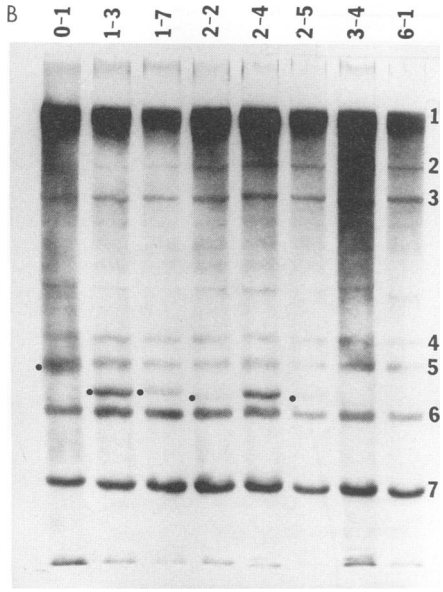

FIG. 3. Replication of 3′-deletion clones. (A) Structure of DIssF and the 3′-deletion clones. (B) RNA electrophoresis of 3′-deletion clones. Intracellular viral RNAs from P0 cells were analyzed. DNAs used to transfect virus-infected cells in each lane are indicated. Dots indicate DI RNAs. Numbers represent A59-specific mRNAs.

the deletion clones showed that the smallest replicating DI RNA construct, DF5′Δ6-9, contains the entire domain I (859 nucleotides) plus the first 135 nucleotides of domain II of DIssF, which is derived from nucleotides 3113 to 3247 from the 5′ end of the MHV JHM genome (13). The next smallest clone, DF5′Δ7-7, which could not replicate, contains the entire domain I plus only 83 nucleotides from domain II. These results demonstrated that the DI RNA requires two discontiguous regions of sequences at its 5′ end for its replication: one at the 5′ terminus, and the other at approximately 3.1 kb from the 5′ end of the genome. These two stretches of sequences were found in all naturally occurring MHV DI RNAs, including those of JHM and A59 strains (4, 21, 23, 34). These two domains are adjacent in DIssE and DIssF but are separated by more than 2 kb in an A59 DI RNA (34) and MHV genomic RNA, suggesting that spacing between the two domains is not important for RNA replication.

Replication signal at the 3′ end of DI RNA. The sequence requirement at the 3′ end was investigated by using constructs which have nested-set deletions starting in domain IV of DIssF and extending toward the 3′ terminus of RNA (Fig. 3A). DF3′Δ0-1, DF3′Δ1-7, DF3′Δ1-3, DF3′Δ2-4, DF3′Δ2-5, and DF3′Δ2-2 yielded RNAs of the expected sizes in P0 cells. Although the amounts of RNA yielded by DF3′Δ2-2 and DF3′Δ2-5 were barely detectable in Fig. 3B, they were reproducibly detected in repeated experiments (data not shown). In contrast, DF3′Δ3-4 and DF3′Δ6-1 did not replicate (Fig. 3B). These two constructs did not produce detectable RNAs even after two serial virus passages in tissue culture (data not shown). DF3′Δ2-2, which was the smallest clone retaining the replicating ability, contains the last 436 nucleotides [excluding the poly(A) tail] from the 3′ end of the MHV JHM genomic RNA. DF3′Δ3-4, which did not replicate, contains the last 378 nucleotides of the same region. Thus, nucleotides 378 to 436 from the 3′ end probably contained at least part of the 3′-end replication signal. The efficiencies of replication of the 3′-end deletion mutants, like their 5′-end deletion counterparts, varied from clone to clone without correlation with the lengths of the 3′-end sequences. For instance, DF3′Δ2-4 replicated more efficiently than did a larger construct, DF3′Δ1-7, and a smaller one, DF3′Δ2-5. Therefore the secondary structure formed by the replication signal at both ends might play an important role in determining the RNA replication efficiency.

Additional internal deletions in the 5′ or 3′ end abrogated replication. The serial deletion studies showed that approximately 994 nucleotides at the 5′ end and 436 nucleotides at the 3′ end, were required for DI RNA replication. To determine whether the entire sequences within the 5′ and 3′ ends were required for RNA replication, we made internal deletions on the replication-competent constructs described

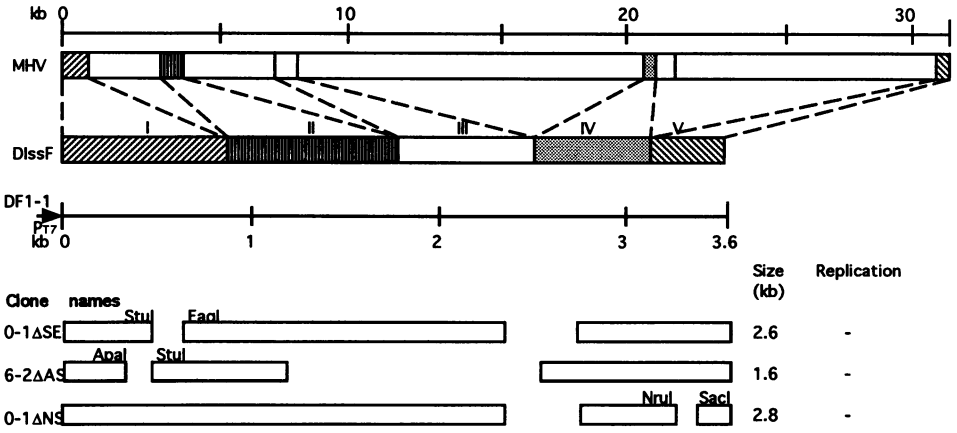

FIG. 4. Structure and replication of clones with additional internal deletions in the 5′ or 3′ end.

above. For the 5′-end region, 221 nucleotides was removed from domain I of DF3′Δ0-1, and 229 nucleotides was removed from DF5′Δ6-2, resulting in 0-1ΔSE and 6-2ΔAS, respectively (Fig. 4). Neither of these two mutants replicated (data not shown). For the 3′-end region, 188 nucleotides of domain V was deleted from DF3′Δ0-1 (Fig. 4). The resulting clone, 0-1ΔNS, also did not replicate (data not shown). The failure of 6-2ΔAS to replicate was not due to its small size (1.6 kb), since a smaller clone, ADI-2 (1.5 kb), replicated (see below). Therefore, we concluded that most of the sequences in the 5′ and 3′ ends defined by serial deletion studies are required for RNA replication. However, we cannot rule out the possibility that small stretches of nucleotides may be deleted without affecting replication.

A 5′–3′-end concatenated clone could replicate. Since the minimum 5′- and 3′-end sequences determined above were made separately on clones which contained longer 3′- or 5′-end sequences, respectively, it was not clear whether a concatenated clone containing the minimum sequences at both ends, i.e., the 5′ end of DF5′Δ6-9 and the 3′ end of DF3′Δ2-2, could replicate. To this end, we made a concatenated mutant, ADI-2, which contained nucleotides 1 to 1089 at the 5′ end and 3092 to 3558 plus the poly(A) tail at the 3′ end of the DIssF sequence (Fig. 5A). The expected RNA product from this clone was 1.5 kb, smaller than that of any other deletion mutants constructed thus far. An RNA species of the expected size was detected when ADI-2 cDNA was transfected into the cells (Fig. 5B), indicating that this concatenated clone, which represents a minimum replicon of MHV, was able to replicate. However, in contrast to other

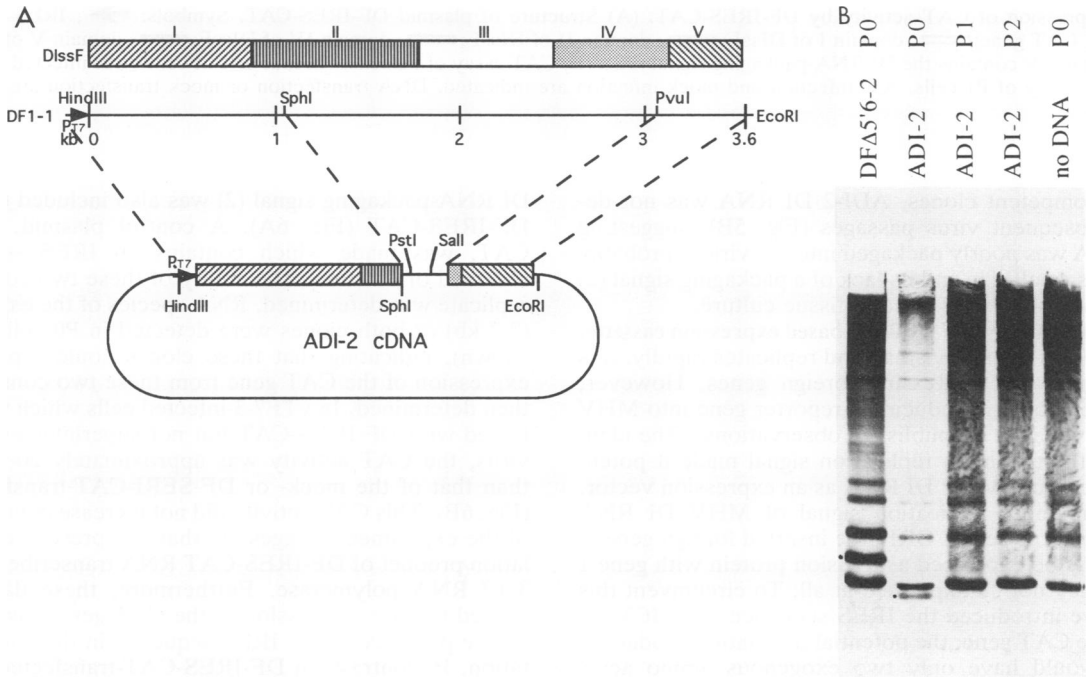

FIG. 5. Replication of the concatenated clone, ADI-2. (A) Structure of ADI-2. (B) RNA electrophoresis of ADI-2 of various passages, as indicated above the lanes. Dots indicate DI RNAs.

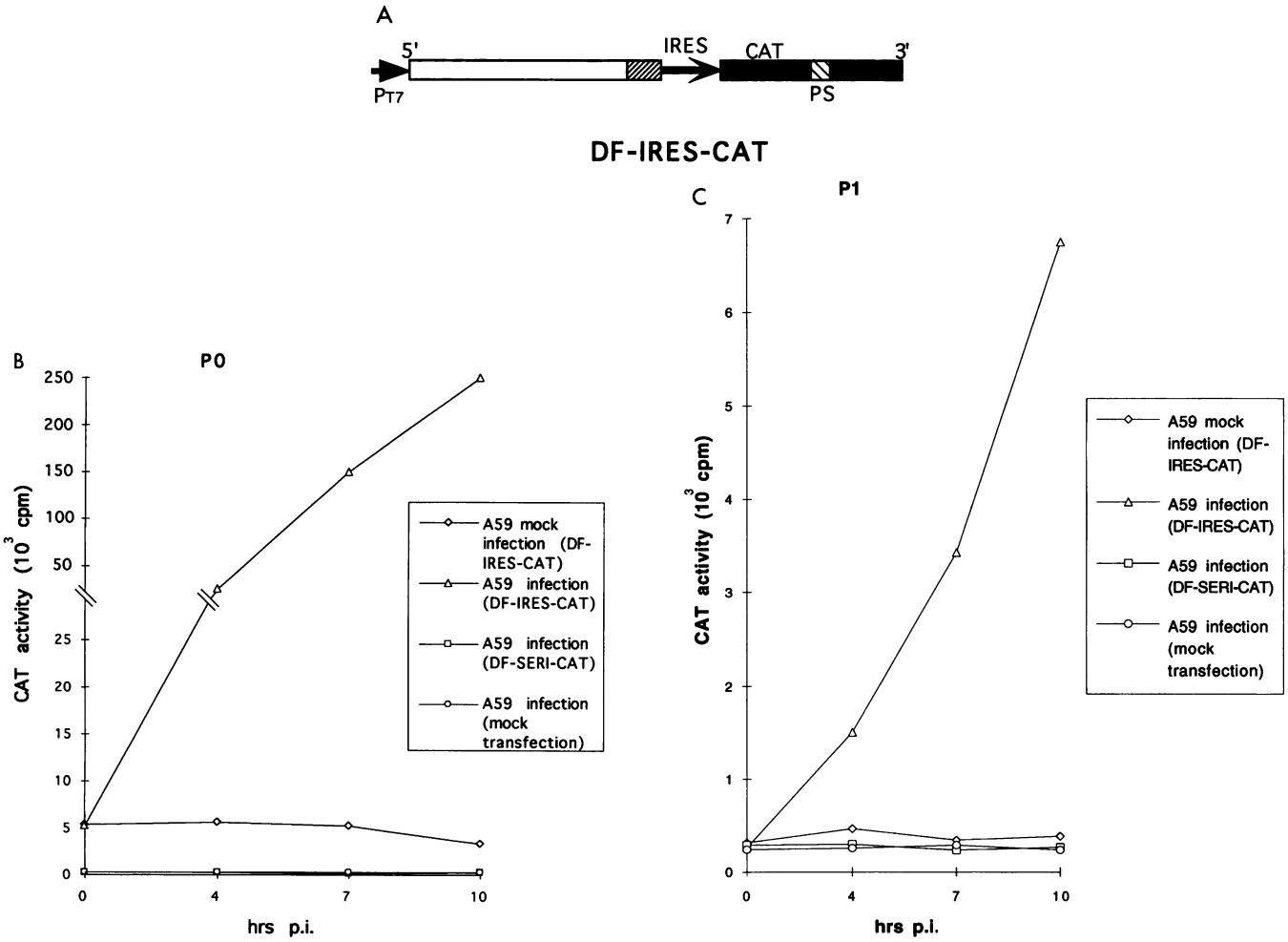

FIG. 6. Expression of CAT activity by DF-IRES-CAT. (A) Structure of plasmid DF-IRES-CAT. Symbols: ➔, IRES sequence of EMCV; ▬, CAT gene; ▭, domain I of DIssF; ▨, domain II of DIssF; ▭, domain IV of DIssF; ▬, domain V of DIssF (23). Note that domain IV contains the DI RNA-packaging signal (PS). (B) CAT assay of P0 cells. All four sets of cells were infected with vTF7-3 first. (C) CAT assay of P1 cells. A59 infection and mock infection are indicated. DNA transfection or mock transfection are indicated in parentheses.

replication-competent clones, ADI-2 DI RNA was not detected in subsequent virus passages (Fig. 5B), suggesting that this RNA was poorly packaged into the virion, probably because of its small size and its lack of a packaging signal (2) and thus could not be passaged in tissue culture.

Construction of an MHV DI RNA-based expression cassette. Since DI RNA is relatively small and replicates rapidly, it is an ideal vehicle for expressing foreign genes. However, previous attempts at introducing a reporter gene into MHV DI RNAs have failed (unpublished observations). The identification of the minimum replication signal made it potentially feasible to use MHV DI RNA as an expression vector. Since the minimum replication signal of MHV DI RNA includes part of the gene 1 ORF, the inserted foreign gene in this RNA may be expressed as a fusion protein with gene 1 product or may not be expressed at all. To circumvent this drawback, we introduced the IRES sequence of EMCV (6) in front of the CAT gene; the potential translation product of this clone would have only two exogenous amino acids derived from the pTM1 vector (27), which is followed by the CAT protein sequence. Further, the previously determined DI RNA-packaging signal (2) was also included to generate DF-IRES-CAT (Fig. 6A). A control plasmid, DF-SERI-CAT, was made which contains an IRES sequence in reversed orientation. The ability of these two constructs to replicate was determined. RNA species of the expected size (2.7 kb) of both clones were detected in P0 cells (data not shown), indicating that these clones could replicate. The expression of the CAT gene from these two constructs was then determined. In vTF7-3-infected cells which were transfected with DF-IRES-CAT but not superinfected with A59 virus, the CAT activity was approximately 20-fold higher than that of the mock- or DF-SERI-CAT-transfected cells (Fig. 6B). This CAT activity did not increase over the course of the experiment, suggesting that it represented the translation product of DF-IRES-CAT RNA transcribed by vTF7-3-T7 RNA polymerase. Furthermore, these data demonstrated that the expression of the CAT gene was dependent on the presence of the IRES sequence in the correct orientation. In contrast, in DF-IRES-CAT-transfected and A59-infected cells, the CAT activity steadily increased following A59 infection; at 10 h p.i. the CAT activity was more than

40-fold greater than that at 0 h p.i. (Fig. 6B). These results taken together indicate that the increased CAT activity in A59-infected cells was due to DF-IRES-CAT RNA replication.

To determine whether the CAT-encoding DI RNA could be packaged into virions and passaged on subsequent viral infections, we harvested virus released from P0 cells and used it to infect another set of cells. As shown in Fig. 6C, P0 virus derived from DF-IRES-CAT-transfected cells yielded an increase of CAT activity of approximately 26-fold at 10 h after reinfection, although the overall level of RNA synthesis was approximately 20-fold lower than that of the original passage (P0 RNA). This lower CAT activity was probably because the DI RNA was not amplified by T7 RNA polymerase in P1 cells prior to or during infection; therefore the amount of transfected RNA in the cells was very small. Nevertheless, the increase of CAT activity represented entirely DI RNA replication. By comparison, viruses derived from either mock- or DF-SERI-CAT-transfected P0 cells and A59 mock-infected, DF-IRES-CAT-transfected P0 cells had only background CAT activity in P1 cells. Therefore we concluded that the MHV DI RNA-based expression vector, DF-IRES-CAT, could mediate CAT gene expression and could be serially passaged, albeit at low efficiency, by virus in tissue culture.

DISCUSSION

In this study, we have used a T7 RNA polymerase-recombinant vaccinia virus-based system to carry out deletion mapping analysis of the replication signal of an MHV DI RNA. This system is sensitive enough to allow detection of DI RNA replication in P0 cells. This avoided the necessity of performing virus passages before the detection of DI RNA replication. Because of frequent recombination and selection occurring between MHV DI and helper viral RNAs (4, 9, 10, 35), virus passages often resulted in DI RNAs which did not represent the original input DI RNA but, rather, represented recombinant RNAs. This is particularly true for RNAs with a poorer replicating ability. The experimental approach used in this study allowed us to detect even RNAs which do not replicate efficiently and permitted quantitative comparison of the replicating abilities of different DI RNAs without being biased by recombination and subsequent selections.

The sequence requirement for MHV DI RNA replication defined in this work includes the first 859 nucleotides from the 5′ end, the last 436 nucleotides from the 3′ end, and, surprisingly, a 135-nucleotide stretch from domain II of DIssF, which is discontiguous from the 5′- and 3′-end sequences on the MHV genome. This requirement of discontiguous sequences for replication has previously been demonstrated in an *E. coli* RNA phage, Qβ, in which a stretch of approximately 100 nucleotides from the middle of Qβ RNA is required for RNA replication (8, 26). Presumably, this middle region in Qβ RNA is bound by ribosomes for initiation of translation. Ribosomes then move along Qβ RNA for protein elongation and at the same time open up secondary structures which block RNA replication. The function of the middle stretch of JHM DI RNA in RNA replication is currently unknown. One possibility is that it serves as a "hinge" sequence which allows the interaction between the 5′- and 3′-end sequences to maintain appropriate secondary structures of JHM DI RNAs for recognition by viral polymerase. Another possibility is that, similar to Qβ RNA, this sequence interacts with host or viral factors to unwind RNA secondary structure. Yet another possibility is that it serves as a replication enhancer element that enhances the replication efficiency of DI RNA.

Our results showed that replication efficiencies varied among the deletion mutants studied, without obvious correlation with the length of either the 5′- or 3′-end sequence. For example, some constructs containing longer 5′- and 3′-end sequences replicated less efficiently than the smaller clones did. It is possible that some RNA regions contain inhibitory sequences. However, it is more likely that RNA sequences of different lengths altered the overall RNA secondary structure and thus interfered with the ability of RNA to interact with components of replication machinery. This possibility may also explain the failure of previous attempts to make replication-competent deletion mutants of DIssE RNA, which may have very rigid RNA structures so that deletion of any sequence results in gross perturbation of secondary structure of replication signals. Therefore, it is possible that the minimum sequence requirements for different DI RNAs and nondefective MHV genomic RNA are different, since the overall RNA structures of different RNAs are likely to be different.

DIssF contains a single ORF spanning from nucleotides 206 through 1708 (23). It has previously been shown that DI RNAs with a long ORF have an evolutionary advantage when competing against DI RNAs with a shorter ORF (1, 9). However, the presence or absence and the length of ORFs of MHV DI RNAs do not affect directly the efficiency of RNA replication (9, 15). Among the deletion clones used in our study, all of the 5′-deletion clones except DF5′Δ0-4 have a truncated ORF, whereas the ORFs of all of the 3′-deletion clones remain intact. In contrast, the ORF of ADI-2 was truncated by the insertion of exogenous cloning sites. Our study showed that the replication efficiencies of DI RNAs do not correlate with the sizes of their ORFs.

Our studies also demonstrated that MHV DI RNA can be used as a vector to express a foreign gene. This utility is similar to DI RNAs described for other viruses (16, 29, 31). In those systems, the CAT gene was usually constructed behind noncoding sequences so that translation of the CAT gene-containing RNA initiated at the first AUG codon of the CAT gene. In contrast, the replication signal of MHV DI RNA includes part of the coding sequence of gene 1a; therefore, a CAT gene constructed behind these sequences would have been translated as a fusion protein with gene 1a protein of MHV. The use of the IRES sequence of EMCV in our construct allowed the expression of the CAT gene efficiently and as a nonfused product. Furthermore, the inclusion of a packaging signal in our DI vector allowed the CAT-encoding DI RNA to be serially passaged. However, the efficiency of DI RNA packaging appears to be very low since the CAT activity of the vector decreased after one virus passage (Fig. 6C). The inefficiency of this identified packaging signal can also be noted from the published data (2, 34). Furthermore, the MHV DI RNA vector can potentially be altered by RNA recombination during virus passage. This MHV DI RNA-based expression system represents the first MHV-derived expression vector. Its utility will be enhanced by overcoming the current shortcomings in packaging efficiency and potential occurrence of RNA recombination.

ACKNOWLEDGMENTS

We thank Stanley Tahara and Eckard Wimmer for generously providing IRES sequence-containing plasmids. We thank Stephen Stohlman for his advice and instructions on manipulating vaccinia

virus. We also thank Mei Chao and John Polo for their helpful discussions and valuable suggestions.

This work was supported by grant AI 19244 from the National Institutes of Health. M. M. C. Lai is an Investigator of Howard Hughes Medical Institute.

REFERENCES

1. **de Groot, R. J., R. G. van der Most, and W. J. M. Spaan.** 1992. The fitness of defective interfering murine coronavirus DI-a and its derivatives is decreased by nonsense and frameshift mutations. J. Virol. **66**:5898–5905.
2. **Fosmire, J. A., K. Hwang, and S. Makino.** 1992. Identification and characterization of a coronavirus packaging signal. J. Virol. **66**:3522–3530.
3. **Fuerst, T. R., E. G. Niles, F. W. Studier, and B. Moss.** 1986. Eucaryotic transient-expression system based on recombinant vaccinia virus that synthesizes bacteriophage T7 RNA polymerase. Proc. Natl. Acad. Sci. USA **83**:8122–8126.
4. **Furuya, T., T. B. MacNaughton, N. La Monica, and M. M. C. Lai.** 1993. Natural evolution of coronavirus defective-interfering RNA involves RNA recombination. Virology **194**:408–413.
5. **Hirano, N., K. Fujiwara, S. Hino, and M. Matsumoto.** 1974. Replication and plaque formation of mouse hepatitis virus (MHV-2) in mouse cell line DBT culture. Arch. Gesamte Virusforsch. **44**:298–302.
6. **Jang, S. K., M. V. Davies, R. J. Kaufman, and E. Wimmer.** 1989. Initiation of protein synthesis by internal entry of ribosomes into the 5′ nontranslated region of encephalomyocarditis virus RNA in vivo. J. Virol. **63**:1651–1660.
7. **Jeong, Y. S., and S. Makino.** 1992. Mechanism of coronavirus transcription: duration of primary transcription initiation activity and effects of subgenomic RNA transcription on RNA replication. J. Virol. **66**:3339–3346.
8. **Kamen, R. I.** 1975. Structure and function of the Qβ RNA replicase, p. 203–234. *In* N. D. Zinder (ed.), RNA phages. Cold Spring Harbor Laboratory, Cold Spring Harbor, N.Y.
9. **Kim, Y.-N., M. M. C. Lai, and S. Makino.** 1993. Generation and selection of coronavirus defective interfering RNA with large open reading frame by RNA recombination and possible editing. Virology **194**:244–253.
10. **Koetzner, C. A., M. M. Parker, C. S. Ricard, L. S. Sturman, and P. S. Masters.** 1992. Repair and mutagenesis of the genome of a deletion mutant of the coronavirus mouse hepatitis virus by targeted RNA recombination. J. Virol. **66**:1841–1848.
11. **Lai, M. M. C.** 1990. Coronavirus: organization, replication, and expression of genome. Annu. Rev. Microbiol. **44**:303–333.
12. **Lai, M. M. C., and S. A. Stohlman.** 1978. RNA of mouse hepatitis virus. J. Virol. **26**:236–242.
13. **Lee, H.-J., C.-K. Shieh, A. E. Gorbalenya, E. V. Koonin, N. La Monica, J. Tuler, A. Bagdzhadzhyan, and M. M. C. Lai.** 1991. The complete sequence (22 kilobases) of murine coronavirus gene 1 encoding the putative protease and RNA polymerase. Virology **180**:567–582.
14. **Leibowitz, J. L., S. R. Weiss, E. Paavola, and C. W. Bond.** 1982. Cell-free translation of murine coronavirus RNA. J. Virol. **143**:905–913.
15. **Liao, C.-L., and M. M. C. Lai.** Unpublished observations.
16. **Luytjes, W., M. Krystal, M. Enami, J. D. Parvin, and P. Palese.** 1989. Amplification, expression, and packaging of foreign gene by influenza virus. Cell **59**:1107–1113.
17. **Mackett, M., G. L. Smith, and B. Moss.** 1985. The construction and characterization of vaccinia virus recombinants expressing foreign genes, p. 191–211. *In* D. M. Glover (ed.), DNA cloning, vol. 2. IRL Press, Oxford.
18. **Makino, S., N. Fujioka, and K. Fujiwara.** 1985. Structure of the intracellular defective viral RNAs of defective interfering particles of mouse hepatitis virus. J. Virol. **54**:329–336.
19. **Makino, S., M. Joo, and J. K. Makino.** 1991. A system for study of coronavirus mRNA synthesis: a regulated, expressed subgenomic defective interfering RNA results from intergenic site insertion. J. Virol. **65**:6031–6041.
20. **Makino, S., C.-K. Shieh, J. G. Keck, and M. M. C. Lai.** 1988. Defective-interfering particles of murine coronavirus: mechanism of synthesis of defective-interfering viral RNAs. Virology **163**:104–111.
21. **Makino, S., C.-K. Shieh, L. H. Soe, S. C. Baker, and M. M. C. Lai.** 1988. Primary structure and translation of a defective interfering RNA of murine coronavirus. Virology **133**:9–17.
22. **Makino, S., F. Taguchi, and K. Fujiwara.** 1984. Defective interfering particles of mouse hepatitis virus. Virology **166**:550–560.
23. **Makino, S., K. Yokomori, and M. M. C. Lai.** 1990. Analysis of efficiently packaged defective interfering RNAs of murine coronavirus: localization of a possible RNA-packaging signal. J. Virol. **64**:6045–6053.
24. **Manaker, R. A., C. V. Piczak, A. A. Miller, and M. F. Stanton.** 1961. A hepatitis virus complicating studies with mouse leukemia. J. Natl. Cancer Inst. **27**:29–51.
25. **McMaster, G. K., and G. G. Carmichael.** 1977. Analysis of single- and double-stranded nucleic acids on polyacrylamide and agarose gels by using glyoxal and acridine orange. Proc. Natl. Acad. Sci. USA **74**:4835–4838.
26. **Meyer, F., H. Weber, and C. Weissmann.** 1981. Interactions of Qβ replicase with Qβ RNA. J. Mol. Biol. **153**:631–660.
27. **Moss, B., O. Elroy-Stein, T. Mizukami, W. A. Alexander, and T. R. Fuerst.** 1990. New mammalian expression vectors. Nature (London) **348**:91–92.
28. **Pachuk, C. J., P. J. Bredenbeek, P. W. Zoltick, W. J. M. Spaan, and S. R. Weiss.** 1989. Molecular cloning of the gene encoding the putative polymerase of mouse hepatitis virus, strain A59. Virology **171**:141–148.
29. **Park, K. H., T. Huang, F. F. Correia, and M. Krystal.** 1991. Rescue of a foreign gene by Sendai virus. Proc. Natl. Acad. Sci. USA **88**:5537–5541.
30. **Pattnaik, A. K., L. A. Ball, A. W. LeGrone, and G. W. Wertz.** 1992. Infectious defective interfering particles of VSV from transcripts of a cDNA clone. Cell **69**:1011–1020.
31. **Percy, N., W. S. Barclay, M. Sullivan, and J. W. Almond.** 1992. A poliovirus replicon containing the chloramphenicol acetyltransferase gene can be used to study the replication and encapsidation of poliovirus RNA. J. Virol. **66**:5040–5046.
32. **Siddell, S.** 1983. Coronavirus JHM: coding assignments of subgenomic mRNAs. J. Gen. Virol. **64**:113–125.
33. **Stohlman, S. A., R. S. Baric, G. N. Nelson, L. H. Soe, M. L. Welter, and R. J. Deans.** 1988. Specific interaction between coronavirus leader RNA and nucleocapsid protein. J. Virol. **62**:4288–4295.
34. **van der Most, R. G., P. J. Bredenbeek, and W. J. M. Spaan.** 1991. A domain at the 3′ end of the polymerase gene is essential for encapsidation of coronavirus defective interfering RNAs. J. Virol. **65**:3219–3226.
35. **van der Most, R. G., L. Heijnen, W. J. M. Spaan, and R. J. de Groot.** 1992. Homologous RNA recombination allows efficient introduction of site-specific mutations into the genome of coronavirus MHV-A59 via synthetic co-replicating RNAs. Nucleic Acids Res. **20**:3375–3381.
36. **Yokomori, K., N. La Monica, S. Makino, C.-K. Shieh, and M. M. C. Lai.** 1989. Biosynthesis, structure, and biological activities of envelope protein gp65 of murine coronavirus. Virology **173**:683–691.